

The Dynamic Behavior of Frameless ALOHA: Drift Analysis, Throughput, and Age of Information

Andrea Munari *Senior Member, IEEE*, Francisco Lázaro *Senior Member, IEEE*,
Giuseppe Durisi *Senior Member, IEEE*, Gianluigi Liva *Senior Member, IEEE*

Abstract

We study the dynamic behavior of frameless ALOHA, both in terms of throughput and age of information (AoI). In particular, differently from previous studies, our analysis accounts for the fact that the number of terminals contending the channel may vary over time, as a function of the duration of the previous contention period. The stability of the protocol is analyzed via a drift analysis, which allows us to determine the presence of stable and unstable equilibrium points. We also provide an exact characterization of the AoI performance, through which we determine the impact of some key protocol parameters, such as the maximum length of the contention period, on the average AoI. Specifically, we show that configurations of parameters that maximize the throughput may result in a degradation of the AoI performance.

I. INTRODUCTION

WIRELESS sensor networks (WSNs) and Internet of things (IoT) systems often involve a large number of terminals that sense a physical process and report time-stamped status

A. Munari, F. Lázaro, and G. Liva are with the Institute of Communications and Navigation, German Aerospace Center (DLR), 82234 Wessling, Germany (email: {andrea.munari, francisco.lazaroblasco, gianluigi.liva}@dlr.de)

G. Durisi is with the Department of Electrical Engineering, Chalmers University of Technology, Gothenburg, 41296, Sweden (e-mail: durisi@chalmers.se).

This paper was presented in part at the 2021 Asilomar Conference on Signals, Systems, and Computers, Pacific Grove, CA, USA [1].

The authors acknowledge the financial support provided by the Swedish Research Council under grant 2021-04970, and by the Federal Ministry of Education and Research of Germany in the programme of "Souverän. Digital. Vernetzt." Joint project 6G-RIC, project identification number: 16KISK022.

updates to a common receiver. This scenario is relevant in, e.g., environmental monitoring, managing of connected vehicles, and asset tracking, where a primary objective is to maintain an up-to-date record of the status of an observed source. A number of performance metrics related to the notion of information freshness have recently been proposed to quantify the ability of a system to reach this goal [2], [3]. In this context, a prominent role is played by the age of information (AoI) [4], [5], which quantifies the amount of time elapsed since the newest update available at the receiver was generated at the source. AoI has been shown to effectively capture fundamental system behaviors in a number of relevant scenarios [6], [7].

Due to the possibly massive number of battery-powered, low-complexity devices that generate traffic in a sporadic fashion, WSNs and IoT systems typically rely on random access protocols at the medium access control (MAC) layer. In particular, random access strategies based on variations of ALOHA [8], [9] are the de-facto choice in a number of commercial systems [10], [11]. Preliminary insights on the information-freshness trade-offs that emerge in random-access systems were derived in [12], [13]. Specifically, these contributions illustrate that throughput and AoI can be optimized simultaneously under ALOHA policies by properly tuning the channel access probability. Further improvements in ALOHA-based protocols with feedback were discussed in [14], [15]. The demand for efficient medium access control strategies for emerging massive WSNs and IoT systems has originated a revived interest in the design of powerful random access protocols [16]–[22]. Among various modern random access approaches, advanced ALOHA-based schemes [17], [23]–[27] gained popularity thanks to their remarkable performance that is achievable with a limited complexity from a signal processing viewpoint. Such protocols allow terminals to transmit multiple copies of their packets over time, and employ successive interference cancellation at the receiver to resolve collisions. This leads to significant throughput improvements, which make these solutions excellent candidates for next-generation IoT networks. Unfortunately, little is known about the behavior of modern random access protocols in terms of information freshness. The first results in this direction were presented in [28], where the focus was on irregular repetition slotted ALOHA [17]. There, non-trivial trade-offs between throughput and average AoI were revealed.

Among advanced ALOHA-based random access protocols, frameless ALOHA [24], [29] emerges as the only variant that is explicitly designed by taking into account the availability of a feedback channel. While the protocols introduced in [17], [25] can be placed in strong connection with the theory of low-density parity-check codes [30], frameless ALOHA operates

instead according to the same principle as rateless codes [31], and has emerged as a particularly promising approach. Specifically, frameless ALOHA allows terminals to transmit copies of their packets over a contention period whose duration is dynamically tuned by the receiver based on the fraction of currently unresolved collisions. A throughput analysis of frameless ALOHA was proposed in [32], which is based on the Markovian analysis of the peeling decoder for LT codes [33]. Both the original analysis of frameless ALOHA [24], [29] and its exact finite-length characterization [32] focus on the *static* behavior of the protocol, i.e., they condition the analysis on the number of terminals becoming active in the current contention period. It follows that the analyses of [24], [29], [32] do not characterize the *dynamic* behavior of the protocol. It is known that ALOHA-like protocols with feedback possess a rich dynamic behavior, which (depending on the load and on the retransmission policy) may result in systems operating in undesirable throughput / delay regimes [34], [35].

Contributions: In this paper, we analyze the dynamic behavior of frameless ALOHA. In contrast to previous works, which assume a fixed number of contending users, we focus on a more general and realistic setup in which the number of users accessing the channel may vary over time, driven by the duration of previous contention periods. We track the dynamic evolution of the system by means of a Markovian analysis, deriving its stationary throughput as well as identifying the stable and unstable operating points of the protocol via a drift study. Moreover, we provide an exact characterization of the average AoI performance of frameless ALOHA as a function of the system parameters. From a technical perspective, the novelty of our contribution lies in the identification of a natural way to model the evolution of the system under analysis and of a convenient parametrization for the corresponding finite-state machine.

The analysis reveals a fundamental trade-off between the AoI and the throughput performance of frameless ALOHA, highlighting the critical role played by some key protocol parameters, such as the maximum length of the contention period. It also shows that operating the system at maximum throughput comes at the expense of an AoI degradation—a trade-off that is fundamentally different from what previously noted for traditional ALOHA strategies. We complement the analysis by introducing simple modifications to the frameless ALOHA protocol, which improve the AoI/throughput trade-off.

Paper Outline: The paper is organized as follows. In Section II, we introduce the system model, and provide basic definitions. The finite-length analysis of the successive interference cancellation (SIC) process for frameless ALOHA is outlined in Section III. The analysis of

the throughput of frameless ALOHA, accounting for the system dynamic behavior, is derived in Section IV. In Section V, we characterize the AoI of frameless ALOHA and illustrate the throughput vs. AoI trade-off via some numerical examples. Conclusions follow in Section VI.

II. SYSTEM MODEL AND PRELIMINARIES

We focus on a system in which U users share a wireless channel to communicate with a common receiver (sink). Time is divided in slots of fixed duration, equal to the length of a packet, and all terminals are slot-synchronous. The medium is shared among all users following a grant-free approach, and a collision channel model is assumed. Specifically, the transmission of two or more packets over a slot leads to a destructive collision, which prevents immediate retrieval of all colliding packets at the sink. On the contrary, packets sent over *singleton slots* are always decoded correctly.

Channel access is regulated by the frameless ALOHA protocol [24], which operates in successive contention periods (CPs) of not necessarily equal length. The receiver initiates a new CP by broadcasting a beacon, whose duration is considered negligible throughout our analysis. After this, every user with data to send, attempts transmission of its packet over each subsequent slot with probability q , potentially sending multiple copies of the same packet over the CP. Conversely, users that do not have a packet to send at the time of beacon reception, refrain from accessing the channel for the whole duration of the CP. The procedure continues until a new beacon sent by the sink notifies the end of the current CP and the start of the next one.

At the receiver side, the decoding of a packet over a singleton slot triggers SIC. Specifically, the interference contribution of all the copies of the retrieved packet is removed, possibly leading to new singleton slots and thus to the decoding of previously collided packets. Note that, in order to implement this procedure, the sink needs to know the position of all the replicas of a packet. This can be achieved, for instance, by using a hash function of the payload as seed for a pseudo-random generator, used by the transmitter to determine the slots of the CP over which to transmit. Upon decoding the payload, the sink becomes thus aware of all the slots occupied by the user, effectively allowing the removal of the interference of that user throughout the CP.

The receiver proceeds with this operation mode on a slot-by-slot basis, and terminates the CP when either all transmitting users have been decoded or a maximum number d_{\max} of slots has been reached. Details on how the sink can determine whether all users have been decoded will

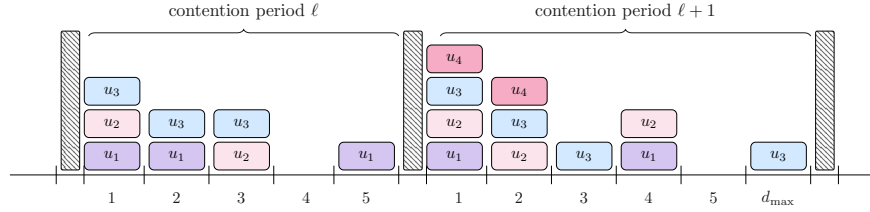


Fig. 1. Example of operations for frameless ALOHA over two successive CPs. We assume $U = 4$ users in the system and a maximum contention duration of $d_{\max} = 6$ slots. Within the ℓ -th CP, only three users are active. The receiver decodes the first packet in slot 5, retrieving the status update of user u_1 . By removing its interference contribution from slot 2, the sink can then decode the packet of user u_3 . Finally, after removing the interference caused by user 3, the sink can also obtain the packet of user 2. Having decoded all users, the sink sends a new beacon at the end of slot 5, initiating the next CP. All four users attempt transmission. The first decoding occurs at slot 3, leading to the retrieval of u_3 . The removal of such packet from slot 2, however, does not resolve completely the existing collision, and SIC stops. The situation does not change after slot 4 (collision not involving u_3), slot 5 (idle), or slot 6, which contains the transmission of a resolved user, and the receiver terminates the CP as the maximum number of slots has been reached, even if some users (i.e., u_1, u_2 and u_4) have not been decoded. Note that the first slot of each CP is used by all active users to send a packet, allowing the sink to infer when complete decoding has occurred (see Section II-A).

be presented in Section II-A. An example of the frameless-ALOHA operations is discussed in Fig. 1.

As to traffic profile, we assume every user to independently generate a new packet over each slot with probability γ . This packet is stored in a one-packet-sized buffer for later delivery. A pre-emption policy with replacement in waiting is implemented, so that, at any given time instant, a user either has one packet to send (the last generated one) or has an empty buffer. Accordingly, a user will attempt transmission over a CP only if it has generated at least one packet over the previous CP. Assuming this lasted for d slots, an arbitrary user has then a packet to transmit with probability

$$\gamma_d := 1 - (1 - \gamma)^d. \quad (1)$$

All copies of the packet sent by each user during a CP are marked with a common time stamp, set to the start time of the CP. Finally, no retransmissions are considered: if a packet is not decoded during the CP it is sent over, it is simply discarded. Recalling that all users are assumed to generate traffic independently, the number U of users that become active at the end of a CP of d slots is thus a binomial random variable with parameters (U, γ_d) . In the remainder of the paper,

we shall denote its probability mass function (PMF) as

$$P_{U|D}(u|d) := \binom{U}{u} \gamma_d^u (1 - \gamma_d)^{U-u}. \quad (2)$$

In this paper, we are interested in evaluating the ability of the system to maintain an up-to-date record of the state of each user at the sink. To this aim, we consider the AoI $\Delta(t)$ of a generic user,

$$\Delta(t) := t - \sigma(t) \quad (3)$$

where $\sigma(t)$ is the time stamp of the last update received by the sink from the user of interest as of time t . The metric grows linearly over time, and drops each time the receiver successfully decodes a packet from the user under observation. For simplicity, we will assume that these refreshes take place at the end of the CP over which the status update was received, i.e., we do not track the exact slot in which the corresponding packet was decoded.¹ This yields the saw-tooth profile exemplified in Fig. 2. In the remainder, we will focus on the *average age of information (AoI)* $\bar{\Delta}$ [36], defined as

$$\bar{\Delta} := \limsup_{t \rightarrow \infty} \frac{1}{t} \int_0^t \Delta(\tau) d\tau. \quad (4)$$

To complement our study, we also evaluate the performance of the protocol in terms of *expected throughput*, defined as the average number of decoded packets per slot [32], and denoted by S . Furthermore, to explore the dynamic behavior of the contention over time, we resort to a drift analysis, akin to the one often employed in the study of ALOHA systems [37]. Specifically, denote by $U^{(\ell)}$ the number of users contending over the ℓ -th CP. We shall characterize the drift for this quantity, defined as the average difference between the number of users contending over the next CP and the number of users contending over the current CP, given that u users contended over the current CP. Let $\Xi(u)$ denote the drift; we have

$$\Xi(u) := \mathbb{E} [U^{(\ell+1)} - U^{(\ell)} | U^{(\ell)} = u]. \quad (5)$$

¹As will be clarified in Section V, this assumption does not change the fundamental trade-offs of interest, and the analysis can be easily adapted to account for this additional factor.

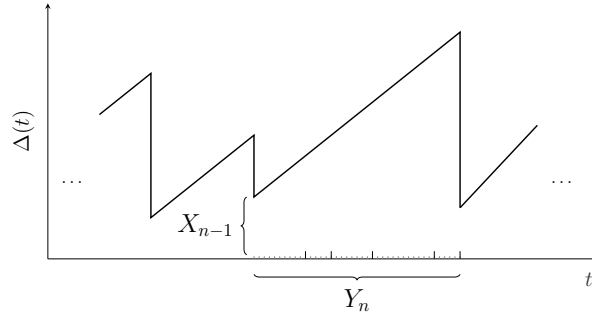


Fig. 2. Evolution over time of the AoI $\Delta(t)$ for a generic user. In the plot, Y_n denotes the duration (in slots) of the n -th inter-update period, possibly composed of multiple CPs. The value at which the AoI is reset upon reception of the node's update that starts the inter-update period is denoted by X_{n-1} , which in our case corresponds to the duration of the CP in which the previous update was received. An in-depth discussion of these quantities will be presented in Section V.

A. Operational Details

We next describe some operational details of the protocol that will be relevant for the subsequent analyses. At the end of each slot, the sink attempts to decode as many users as possible, canceling also their interference. When no more users can be decoded, i.e., when the contention contains no more singleton slots, the receiver decides whether to terminate the CP or not. Specifically, the CP is concluded only if all active users have been decoded, or, alternatively, if a maximum number of slots has elapsed since the beginning of the contention. Note that, without further assumptions, it is in general not possible for the sink to determine whether all active users have been decoded, since the sink cannot discriminate between inactive users, who do not have a packet to transmit, and active users, who do have a packet to transmit, but have not transmitted their packet (yet) since the beginning of the CP.

To allow the sink to determine whether all active users have been decoded, we set the slot access probability to 1 in the first slot of every contention period. This implies that all active users will transmit their packet in the first slot. Furthermore, we make the reasonable assumption that the receiver can distinguish among empty slots, singleton slots containing exactly one packet, and *collided slots* containing two or more packets. Under this assumption, the sink can use the first slot of every CP to determine whether all active users have been decoded or not. In particular, after canceling the interference from a decoded user, the sink can check whether the first slot becomes empty to infer whether there are no more undecoded active users and the CP can be terminated. This strategy allows the receiver also to detect empty CPs. Indeed, these CPs

are characterized by an empty initial slot. Note that the minimum CP duration in our setting is one slot, reached when either no users or a single user have data to transmit.

We emphasize that more realistic and sophisticated methods may be devised to estimate the number of active users in the CP, as discussed for instance in [29]. For the purpose of the analysis provided in this paper, the proposed technique suffices, in the sense that it provides a simple model for the cost (i.e., overhead) required for the estimation of the number of active users.

B. Notation

In the remainder of the paper, we denote a discrete r.v. and its realization using upper-case and lower-case letters such as X and x , respectively, whereas the PMF of a random variable X is indicated by $P_X(x)$. The conditional PMF of X given Y is denoted as $P_{X|Y}(x|y)$. We further write the state of a homogeneous, discrete-time Markov chain at time ℓ as $X^{(\ell)}$, and denote its one-step transition probability from state i to state j as

$$p_X(i, j) := \mathbb{P}\{X^{(\ell+1)} = j \mid X^{(\ell)} = i\}. \quad (6)$$

In the case of bi-dimensional Markov chains, we maintain the same notation, but denote the state by means of a two-element vector, e.g., $j = (j_1, j_2)$.

III. FRAMELESS ALOHA ANALYSIS

Following [32], we model the iterative SIC process at the sink using a finite-state machine. A state is identified by the triplet (w, c, r) , where w denotes the number of unresolved users, c denotes the number of collided slots (ignoring the initial slot), and r is the number of singleton slots. We denote by Pre_d the pre-decoding state, i.e., the state right after the sink observes the d th slot within a CP and before it tries to decode any new packets, whereas Pos_d denotes the post-decoding state, i.e., the state after SIC decoding. Note that, in the pre-decoding state, we always have $r \in \{0, 1\}$, since the reception of a new slot yields at most one new singleton slot. Furthermore, the post-decoding state must have $r = 0$, since all singleton slots result in a successful decoding operation, and the corresponding packet as well as its replicas are removed after SIC. For clarity, in Example 1 we illustrate how the pre- and post-decoding state evolve during a contention.

Example 1 (Pre- and post-decoding state): Consider the first (leftmost) contention period shown in Fig. 1. We have that 3 users are contending. Thus after the initial slot, we have $\text{Pre}_1 = (w = 3, c = 0, r = 0)$, since we have 3 undecoded users, no collided slots (according to our definition, c denotes the number of collided slots *ignoring* the initial one), and no singleton slots. The post decoding state after the first slot is $\text{Pos}_1 = \text{Pre}_1 = (3, 0, 0)$ since no users can be resolved. After receiving the second slot, we have $\text{Pre}_2 = \text{Pos}_2 = (3, 1, 0)$, since this slot is a collision. The third slot is also a collision, thus we have $\text{Pre}_3 = \text{Pos}_3 = (3, 2, 0)$. Upon reception of the fourth slot, we have $\text{Pre}_4 = \text{Pos}_4 = (3, 2, 0)$, since this slot is empty. The fifth slot is a singleton, thus we have $\text{Pre}_5 = (3, 2, 1)$. In this case, this singleton slot allows the receiver to resolve all 3 users relying on SIC. Thus, we have $\text{Pos}_5 = (0, 0, 0)$.

In order to describe the decoding process, we next provide a characterization of the conditional probability of Pos_d given Pre_d and of the conditional probability of Pre_d given Pos_{d-1} .

A. State Initialization

Assume that u users are active. The state is initialized as

$$\text{Pre}_1 = \begin{cases} (0, 0, 0) & \text{if } u = 0 \\ (1, 0, 1) & \text{if } u = 1 \\ (u, 0, 0) & \text{if } u > 1. \end{cases} \quad (7)$$

Note that, when $u > 1$ users are active, we have $c = 0$ although the initial slot is collided. The reason is that c , according to our definition, denotes the number of collided slots ignoring the initial slot.

B. Conditional Probability of Pos_d Given Pre_d

We next derive the conditional probability of the post-decoding state Pos_d given the pre-decoding state $\text{Pre}_d = (w, c, r)$. Two cases need to be distinguished: $r = 0$ and $r = 1$. If $r = 0$, the state remains unchanged since no users can be resolved. Hence, we have

$$\mathbb{P}\{\text{Pos}_d = (w', c', r') | \text{Pre}_d = (w, c, 0)\} = \begin{cases} 1 & \text{if } w' = w, c' = c, r' = 0 \\ 0 & \text{otherwise.} \end{cases} \quad (8)$$

Let us now focus on the case $r = 1$. It is convenient to describe SIC decoding as an iterative process in which one user is resolved at each iteration, potentially resulting in new singleton

slots. As a consequence, r may be larger than 1 during the iterative process. This process is terminated when no singleton slots are available, i.e., $r = 0$. To characterize the state evolution at each SIC iteration, we use [32, Theorem 1]. This theorem, when specialized to the scenario considered here, implies that, if the state is (w, c, r) with $w \geq 1$ and $r \geq 1$, after resolving exactly one user, the state becomes $(w - 1, c - j, r - i + j + a)$ with probability

$$I_w(a) \binom{c}{j} h_w^j (1 - h_w)^{c-j} \binom{r-1}{i-1} \left(\frac{1}{w}\right)^{i-1} \left(1 - \frac{1}{w}\right)^{r-i} \quad (9)$$

for $a \in \{0, 1\}$, $j \in \{0, \dots, c\}$, $i \in \{1, \dots, r-1\}$ and $i - j - a \leq r$, where

$$I_w(a) = \begin{cases} 1, & \text{if } w \neq 2, a = 0 \\ 1, & \text{if } w = 2, a = 1 \\ 0, & \text{otherwise} \end{cases} \quad (10)$$

and with

$$h_w = \frac{\sum_{k=2}^{u-w+2} \Lambda_k k(k-1) \frac{1}{u} \frac{w-1}{u-1} \frac{\binom{u-w}{k-2}}{\binom{u-2}{k-2}}}{1 - \sum_{k=1}^{u-w+1} \Lambda_k w \frac{\binom{u-w}{k-1}}{\binom{u}{k}} - \sum_{k=0}^{u-w} \Lambda_k \frac{\binom{u-w}{k}}{\binom{u}{k}}} \quad (11)$$

where $\Lambda_k = \binom{u}{k} q^k (1-q)^{u-k}$. Here, i accounts for the number of singleton slots that become empty, j accounts for the number of collided slots (ignoring the initial slot) that become singletons, and a takes value 1 when the initial slot becomes a singleton and 0 otherwise.

To derive the desired conditional probability $\mathbb{P}\{\text{Pos}_d = (w', c', 0) | \text{Pre}_d = (w, c, 1)\}$ for all values of w' , and c' , we apply the result just stated iteratively, stopping when we reach a state with no singleton slots.

C. Contention Period Termination

The CP is terminated after $d < d_{\max}$ slots only if all u active users are resolved, i.e., only if the post-decoding state is $\text{Pos}_d = (0, 0, 0)$.² However, when $d = d_{\max}$, the CP is terminated, no matter what the value of $\text{Pos}_{d_{\max}}$ is.

²Note that, although the decoder cannot track w , it can use the initial slot to verify whether $w = 0$.

D. Conditional Probability of Pre_d Given Pos_{d-1}

We now analyze how the state changes when one slot is added to the CP. To do so, we derive the conditional probability of the pre-decoding state Pre_d given the post-decoding state $\text{Pos}_{d-1} = (w, c, 0)$, for $d \geq 2$. Three different cases must be considered, which result in $\text{Pre}_d = (w, c, 0)$, $\text{Pre}_d = (w, c, 1)$, and $\text{Pre}_d = (w, c + 1, 0)$, respectively. In the first case, the d th slot contains no packet from any of the w unresolved³ users. This event, which occurs with probability $(1 - q)^w$, yields a pre-decoding state $\text{Pre}_d = (w, c, 0)$. Hence, we have

$$\mathbb{P}\{\text{Pre}_d = (w, c, 0) | \text{Pos}_{d-1} = (w, c, 0)\} = (1 - q)^w. \quad (12)$$

In the second case, the d th slot contains the packet of exactly one of the w unresolved users. It can then be verified that

$$\mathbb{P}\{\text{Pre}_d = (w, c, 1) | \text{Pos}_{d-1} = (w, c, 0)\} = wq(1 - q)^{w-1}. \quad (13)$$

Finally, in the third case, the d th slot contains the transmission of two or more unresolved users, which yields

$$\mathbb{P}\{\text{Pre}_d = (w, c + 1, 0) | \text{Pos}_{d-1} = (w, c, 0)\} = 1 - (1 - q)^w - wq(1 - q)^{w-1}. \quad (14)$$

In conclusion, we observe that, for a fixed contention period duration d , the state space of the dynamical system defined by the triplet (w, c, r) has cardinality that is upper-bounded by Ud^2 . By examination of the recursions (8) and (9), we can see that, for fixed d , the evaluation of the state probabilities has a complexity that is $\mathcal{O}(U^2d^4)$, i.e., the scaling is quadratic in the number of users, and polynomial in the contention period length. The recursions (12), (13), and (14), instead, bear only a linear dependency on d and on U (the three equations need to be evaluated for $0 \leq c \leq d$ and $0 \leq w \leq U$). While this calculation shows that it might indeed be complex to adopt the analysis for very large user populations and large maximum contention period lengths, the polynomial complexity of the problem still allows one to study the system performance for range of parameters' values that are of interest for practical systems (few hundreds of users, with d_{\max} in the order of few hundreds slots).

³We assume that transmissions from already resolved users are canceled immediately after the reception of the slot. Thus we only consider unresolved users in the pre-decoding state Pre_d .

E. Derivation of Some Useful Quantities

We will next use the state-transition probabilities just introduced to derive three quantities that will turn out important for the characterization of the average AoI.

The first quantity is the probability that the contention period is terminated after exactly d slots, given that the number of active users is u . We denote this quantity by $P_{D|U}(d|u)$. To characterize it, we need to consider three different cases. The first one is $d = 1$. In this case, we have

$$P_{D|U}(1|u) = \begin{cases} 1 & \text{if } u \in \{0, 1\} \\ 0 & \text{otherwise.} \end{cases} \quad (15)$$

The second case covers $d \in \{2, \dots, d_{\max} - 1\}$. Recall that, in this case, the CP is terminated only if all u active users are resolved. Hence,

$$P_{D|U}(d|u) = \mathbb{P}\{\text{Pos}_d = (0, 0, 0)\}. \quad (16)$$

The probability of the remaining case, $d = d_{\max}$, can be easily obtained as

$$P_{D|U}(d_{\max}|u) = 1 - \sum_{d=1}^{d_{\max}-1} P_{D|U}(d|u). \quad (17)$$

The second quantity we are interested in is the conditional probability that exactly m users were decoded at the end of the CP, given that u users were active. We denote this quantity by $P_{M|U}(m|u)$. To characterize it, we must distinguish two cases: $m < u$ and $m = u$. When $m < u$, since not all users were resolved, the CP was terminated after d_{\max} slots. Hence, we have

$$P_{M|U}(m|u) = \sum_{c=1}^{d_{\max}-1} \mathbb{P}\{\text{Pos}_{d_{\max}} = (u - m, c, 0)\}. \quad (18)$$

We consider now the case $m = u$. To obtain $P_{M|U}(u|u)$, we need to add the probabilities of all post-decoding states in which all users are decoded:

$$P_{M|U}(u|u) = \sum_{d=1}^{d_{\max}} \mathbb{P}\{\text{Pos}_d = (0, 0, 0)\} = 1 - \sum_{m=0}^{u-1} P_{M|U}(m|u). \quad (19)$$

The third quantity of interest, which we denote by $\beta(m, u)$, is the conditional probability that m users are resolved, given that u users accessed the CP and that the CP ran until its maximum duration d_{\max} . We can obtain $\beta(m, u)$ by summing the probabilities of all post-decoding states $\text{Pos}_{d_{\max}}$ in which exactly $u - m$ active users are unresolved, and then normalizing by the sum of the probabilities of all states $\text{Pos}_{d_{\max}}$:

$$\beta(m, u) = \frac{\sum_{c=1}^{d_{\max}-1} \mathbb{P}\{\text{Pos}_{d_{\max}} = (u - m, c, 0)\}}{\sum_{w=2}^u \sum_{c=1}^{d_{\max}-1} \mathbb{P}\{\text{Pos}_{d_{\max}} = (w, c, 0)\}}. \quad (20)$$

IV. THROUGHPUT PERFORMANCE

We provide in this section an analysis of the stationary throughput achievable with the frameless ALOHA protocol, which will turn out useful for the characterization of the AoI. Previous works, e.g., [24], [29], [32], [38], have studied the protocol behavior either over a single CP, or under the assumption that the number of contending terminals is fixed. For this scenario, the number of packets that can be decoded under an optimized access probability has been derived. The setting under consideration in this paper, however, is characterized by a richer dynamic, since the number of users accessing the channel, and thus the level of contention, may vary over time. To appreciate this aspect, observe how, for instance, a long CP increases the probability for more users to generate at least one packet over its duration. This leads to a harsher contention over the successive period, which, in turn, is likely to last longer. Similarly, contentions resolved in few slots will instead drive the system on average towards shorter and less loaded CPs.

To capture the impact on throughput of this non-trivial evolution, we start by focusing on the homogeneous Markov processes $D^{(\ell)}$ and $U^{(\ell)}$, tracking the duration of the ℓ -th CP and the number of users contending over it, respectively. Let us first consider the former, which takes values in the set $\{1, \dots, d_{\max}\}$. Recalling that the duration of the $(\ell + 1)$ -th CP is driven by the number of users contending over it, we compute the transition probabilities for the Markov process as

$$p_D(i, j) = \sum_{u=0}^U \mathbb{P}\{D^{(\ell+1)} = j \mid U^{(\ell+1)} = u\} \cdot \mathbb{P}\{U^{(\ell+1)} = u \mid D^{(\ell)} = i\} \quad (21)$$

$$= \sum_{u=0}^U P_{D|U}(j|u) P_{U|D}(u|i) \quad (22)$$

where $P_{U|D}$ is given in (2), and $P_{D|U}$ in (16) and (17). Similarly, the transition probabilities for the Markov process $U^{(\ell)}$ are

$$p_U(i, j) = \sum_{d=1}^{d_{\max}} \mathbb{P}\{U^{(\ell+1)} = j \mid D^{(\ell)} = d\} \cdot \mathbb{P}\{D^{(\ell)} = d \mid U^{(\ell)} = i\} \quad (23)$$

$$= \sum_{d=1}^{d_{\max}} P_{U|D}(j|d) P_{D|U}(d|i). \quad (24)$$

In both cases, it is easy to verify that these finite-state Markov chains are irreducible and aperiodic, and thus ergodic. In the remainder of the paper, we shall indicate their stationary

distributions, derived by solving the corresponding balance equations, as $\pi_D(d)$ and $\pi_U(u)$, respectively.

Let us now denote by $M^{(\ell)}$ the number of successfully decoded users over the ℓ -th CP. Following this notation, the system throughput S , i.e., the *average* number of decoded packets per slot, can be expressed as

$$S = \lim_{t \rightarrow \infty} \frac{\frac{1}{t} \sum_{\ell=1}^t M^{(\ell)}}{\frac{1}{t} \sum_{\ell=1}^t D^{(\ell)}}. \quad (25)$$

Observing that

$$\mathbb{P}\{M^{(\ell)} = m\} = \sum_{u=0}^U P_{M|U}(m|u) \mathbb{P}\{U^{(\ell)} = u\} \quad (26)$$

we conclude that the statistics of $M^{(\ell)}$ can be directly derived from that of the number of contending users over the corresponding CP. Hence, this process also admits a stationary distribution. Accordingly, both the numerator and denominator in (25) admit finite limits for $t \rightarrow \infty$ by virtue of the ergodicity of the involved chains. This allows us to compute S as the ratio of the expected values of the processes in stationary conditions as follows:

$$S = \frac{\sum_{m=0}^U \sum_{u=0}^U m P_{M|U}(m|u) \pi_U(u)}{\sum_{d=1}^{d_{\max}} d \pi_D(d)}. \quad (27)$$

Leaning on this result, we provide in Fig. 3 a first characterization of the behavior of the system. In the plot, we illustrate how the stationary throughput changes as a function of the transmission probability q , for a population of $U = 200$ users, and a CP with maximum duration of $d_{\max} = 250$ slots. The reported results were obtained by setting the activation probability γ such that the average number of users generating a new packet over each slot, γU , equals 0.8. The solid line shows the analytical outcomes obtained by evaluating (27), whereas the markers denote results of Monte Carlo simulations. For the latter, the complete protocol operations, including traffic generation, channel access and SIC procedures over a collision channel were implemented.

The exhibited trend confirms the existence of an optimal, throughput maximizing, medium access probability. Indeed, too low values of q tend to result in successful yet unnecessarily long CPs, where many slots may remain unused. Conversely, when users become too aggressive in their transmission policies, collisions become predominant, leading to the sharp decrease in throughput which is typically observed in grant-free schemes that resort to SIC [17].

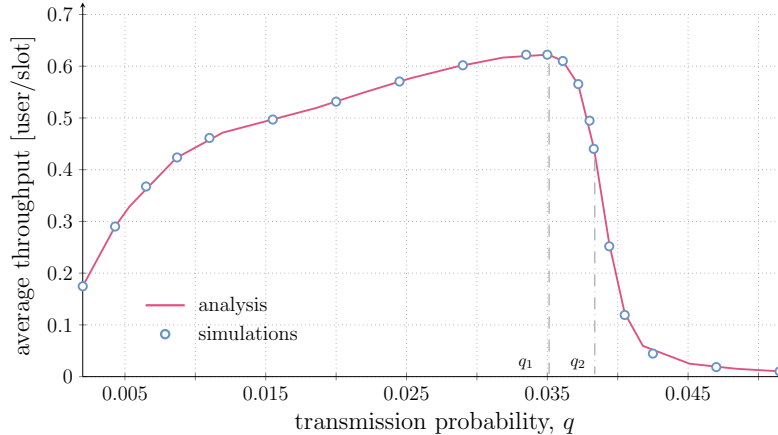


Fig. 3. System throughput S vs transmission probability q . A population of $U = 200$ users and a maximum CP duration of $d_{\max} = 250$ slots are considered. The packet generation probability is set so that $\gamma U = 0.8$.

We remark that the behavior just described is representative of the *average* performance of frameless ALOHA, as captured by the throughput definition in (25). To better appreciate the *finer-grained dynamics* of the protocol, it is useful to resort to a *drift analysis*. Recalling the definition in (5), we are interested in $\Xi(u)$, i.e., the average difference between the number of users contending over the next CP and the number of users contending over the current CP, given that u users contended over the current CP. Leaning on the transition probabilities for the Markov chain $U^{(\ell)}$, the quantity can conveniently be expressed as

$$\Xi(u) = \sum_{i=0}^U i p_U(u, i) - u \quad (28)$$

and easily be computed for every u by resorting to the formulations derived in (24). Interestingly, the drift provides an indication of how the system tends to evolve. Indeed, when $\Xi(u) < 0$ fewer contending users are expected, whereas $\Xi(u) > 0$ denotes a tendency to have more terminals attempting transmission in the upcoming CP. In turn, conditions characterized by $\Xi(u) = 0$ are referred to as *equilibrium points*. This behavior can be conveniently summarized using the diagram reported in Fig. 4, representative of a system with $U = 200$ users and a maximum CP duration of 250 slots.⁴ The plot reports, for any value of u , the average number of users contending over the next CP, i.e., $\Xi(u) + u$ (solid lines). A bisector of the plane (dashed line) is

⁴The analytical results for the stability study were also verified by means of dedicated numerical simulations. The outcomes, which indicate an excellent match, are not reported, to avoid crowding the figure.

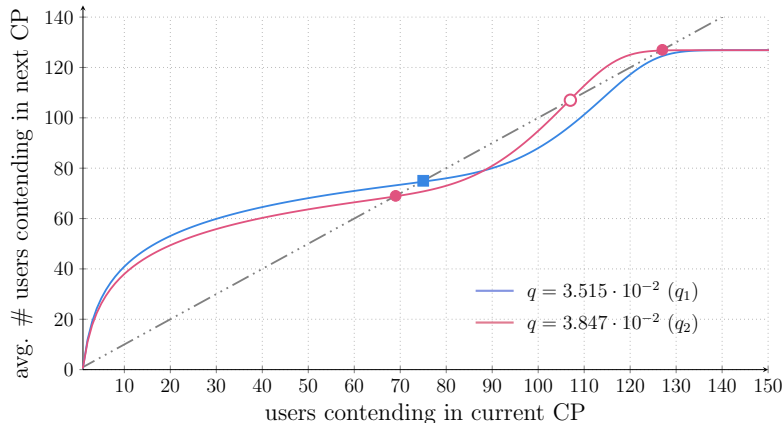


Fig. 4. Graphical illustration of the drift analysis for the system. The plot reports the average number of users expected to access the channel in the next CP as a function of the number of users contending in the current CP (i.e., $\Xi(u)$ vs. u). A population of $U = 200$ users and a maximum CP duration of $d_{\max} = 250$ slots are considered. The packet generation probability is set so that $\gamma U = 0.8$. Two values of q are studied, corresponding to the operating points highlighted in Fig. 3. Filled markers denote stable equilibrium points, whereas the empty marker for the case $q = q_2$ indicates an unstable equilibrium. We note that, in both configurations, the curves saturate to a maximum value of $U(1 - (1 - \gamma)^{d_{\max}}) \simeq 126$, corresponding to the number of users that become active for $\gamma U = 0.8$ when the maximum CP duration is undergone.

also shown, so that for any point on the u -axis, the drift corresponds to the difference between the solid and dashed curves.

Consider first the blue curve, obtained for a transmission probability $q = q_1 = 0.03515$. Such value, also highlighted in Fig. 3, maximizes the average throughput achieved by the protocol for the d_{\max} under study. In this configuration, the drift plot pinpoints the existence of a single equilibrium point, indicated by the square marker and attained for $u \simeq 75$. This behavior is confirmed by the leftmost results in Fig. 5, reporting the stationary distributions for the CP duration (π_D), number of contending users (π_U), and number of decoded users over a CP (π_M). When q is chosen so as to provide the optimal throughput, the contention level is well concentrated around a desired value, with small fluctuations in the CP duration and number of transmitting nodes due to the random nature of the access procedures.

The situation changes drastically when the transmission probability is slightly increased, i.e., if one sets $q = q_2 = 0.03847$. In this case, Fig. 4 (purple curve) reveals the existence of three equilibrium points. The middle one (empty marker) is unstable, in the sense that the system

will tend to move away from it although it expresses a null drift.⁵ Conversely, the leftmost and rightmost ones (filled markers) are stable, and hint at a more complex behavior. This can be appreciated by looking at the stationary distributions on the right part of Fig. 5, which exhibit a bimodal structure. In this case, the system oscillates between a desirable equilibrium, granting a good throughput and characterized by CP durations and number of contending users similar to the ones observed for $q = q_1$, and a detrimental one. In the latter condition, CPs of the maximum duration are experienced, triggering more contention (rightmost peak of π_U) and a lower success rate (leftmost peak of π_M).

From this standpoint, two remarks are in order. First, when operating in the detrimental configuration, the protocol achieves poor throughput, triggering the reduction in the average performance observable in Fig. 3. Second, and perhaps more relevant from a practical perspective, the system may require a long time before returning to the throughput-efficient equilibrium point, once it has reached the undesired equilibrium point. One way to measure this elapsed time is to count the number of slots elapsed on average until the system returns to a favorable configuration after having experienced a CP of the maximum duration. In the setting under study, we declare return to a desired equilibrium as soon as a contention is terminated after less than 150 slots. This value was chosen as representative as it is one of the largest CP durations still lying close to the first peak of the distribution π_D (see Fig. 5). For the considered parameters, this transition takes approximately 14200 slots.⁶ In other words, a period corresponding to roughly 150 CPs of 100 slots—a typical slot duration for the case in which the system is in the desirable equilibrium point—are wasted because the system is stuck in the undesired equilibrium point. In this situation, a reset may be required to shorten the time spent in highly inefficient conditions, with an extra cost in terms of overhead.

To summarize, our study reveals that frameless ALOHA has a complex dynamic behavior, which calls for a careful tuning of the system parameters. In this perspective, the presented analysis offers a useful tool for an initial system design.

⁵Note indeed that, for any u to the left of this equilibrium point, we have positive drift, and the system will tend to move to more contending nodes. Similarly, for any u to the right of the point, $\Xi(u) < 0$, once again drifting away from the equilibrium.

⁶The reported value was obtained by means of a first step analysis of the involved Markov processes. The analytical details, omitted here, follow the same methodology that will be presented in depth in Section V in the context of the AoI study.

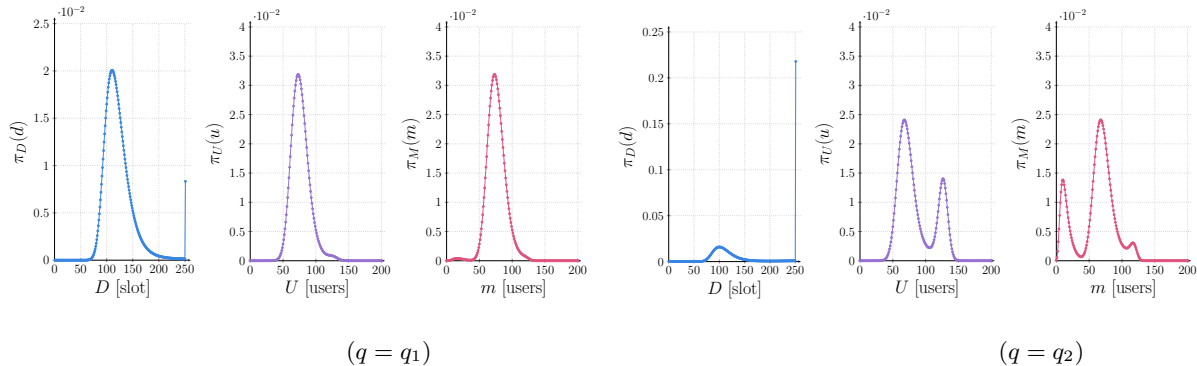


Fig. 5. Stationary distribution of the CP duration, $\pi_D(d)$, number of contending users per CP $\pi_U(u)$, and number of decoded users per CP, $\pi_M(m)$, for the two values of transmission probability q_1 and q_2 . In all cases, results were generated considering $U = 200$, $d_{\max} = 250$, and $\gamma U = 0.8$.

V. AVERAGE AGE OF INFORMATION

We now focus on the characterization of frameless ALOHA in terms of information freshness. To this aim, we provide first some preliminary results that will facilitate the derivation of the average AoI.

Fix a generic user for which the AoI is tracked, and denote by $\nu(u, d)$ the conditional probability that the user delivers a status update over the current CP, given that u users contend and that the CP has a duration of d slots. Consider first the case in which the CP is terminated prior to reaching its maximum length. Recalling the protocol operation, this condition occurs when all contending users are successfully decoded. Accordingly, $\nu(u, d)$ is simply given by the probability for the node of interest to have participated to the contention, given by u/U . Conversely, if the CP runs for d_{\max} slots, the conditional probability for the user to deliver a packet given that m users are successfully decoded can be obtained as $(m/U)\beta(m, u)$, as a consequence of (20). Combining these two results we then have:

$$\nu(u, d) = \begin{cases} \frac{u}{U} & d < d_{\max} \\ \sum_{m=0}^u \frac{m}{U} \beta(m, u) & d = d_{\max}. \end{cases} \quad (29)$$

Next, we introduce an ancillary Markov chain, whose state is defined as $Z^{(\ell)} = (D^{(\ell)}, S^{(\ell)})$. The first component, which we have already discussed, characterizes the duration of the ℓ -th CP, whereas $S^{(\ell)}$ is a binary r.v. taking value 1 if an update from the user of interest has been successfully received over the ℓ -th CP, and taking value 0 otherwise. Consider now the

probability for the chain to transition from state (j, s) to state $(d, 1)$. By definition, this event occurs when the current CP has duration d slots, and the user delivers an update. Observing that the user's success does not depend on its outcome over the previous CP, we can simplify the transition probability to

$$p_Z((j, s), (d, 1)) := \mathbb{P}\{Z^{(\ell+1)} = (d, 1) \mid Z^{(\ell)} = (j, s)\} \quad (30)$$

$$= \mathbb{P}\{S^{(\ell+1)} = 1, D^{(\ell+1)} = d \mid D^{(\ell)} = j\}. \quad (31)$$

Conditioning now on the number of users contending over the CP, we further have

$$\mathbb{P}\{S^{(\ell+1)} = 1, D^{(\ell+1)} = d \mid D^{(\ell)} = j\} \quad (32)$$

$$= \sum_{u=0}^U \mathbb{P}\{S^{(\ell+1)} = 1 \mid U^{(\ell+1)} = u, D^{(\ell+1)} = d\} \cdot \mathbb{P}\{U^{(\ell+1)} = u, D^{(\ell+1)} = d \mid D^{(\ell)} = j\} \quad (33)$$

$$= \sum_{u=0}^U \mathbb{P}\{S^{(\ell+1)} = 1 \mid U^{(\ell+1)} = u, D^{(\ell+1)} = d\} \cdot \mathbb{P}\{D^{(\ell+1)} = d \mid U^{(\ell+1)} = u\} \\ \cdot \mathbb{P}\{U^{(\ell+1)} = u \mid D^{(\ell)} = j\}. \quad (34)$$

Finally, using (29), (2), (16), and (17), we can write $p_Z((j, s), (d, 1))$ compactly as

$$p_Z((j, s), (d, 1)) = \sum_{u=0}^U \nu(u, d) P_{D|U}(d|u) P_{U|D}(u|j). \quad (35)$$

Following similar steps, we can express the transition probabilities from a generic state (j, s) to a state $(d, 0)$ in which the user does not deliver an update as

$$p_Z((j, s), (d, 0)) = \sum_{u=0}^U (1 - \nu(u, d)) P_{D|U}(d|u) P_{U|D}(u|j). \quad (36)$$

It is immediate to verify that the finite-state Markov chain $Z^{(\ell)}$ is irreducible and aperiodic, and admits thus a stationary distribution, which we denote as $\pi_Z(d, s)$.

A. Average AoI Analysis

Let us now compute the average AoI achieved by frameless ALOHA. The metric can be conveniently expressed in terms of the *inter-update time* Y_n and the *system time* X_n , introduced in Fig. 2. The former quantity captures the number of slots elapsed between two successive update deliveries from the node of interest. The latter denotes the time between the generation of an update and its delivery, which, in our case, corresponds to the duration of the CP over

which the update was decoded. With this notation, we have via standard geometrical arguments, see, e.g., [2, Eq. (3)],

$$\bar{\Delta} = \frac{\mathbb{E}[X_n Y_n] + \mathbb{E}[Y_n^2]/2}{\mathbb{E}[Y_n]} \quad (37)$$

under the assumption that (Y_n, X_n) is a stationary ergodic process. In the remainder, we drop for ease of notation the index n denoting a specific update delivery, and focus on the stationary behavior of the quantities of interest.

As initial remark, we observe that the PMF $P_X(x)$ of the system time can be readily computed from the stationary distribution of the Markov chain $Z^{(\ell)}$. We have

$$P_X(x) = \frac{\pi_Z(x, 1)}{\sum_{\delta=1}^{d_{\max}} \pi_Z(\delta, 1)} \quad (38)$$

where the numerator denotes the probability for the system to be in a CP of duration x slots in which the tracked user is decoded, and the denominator is a normalization factor, capturing that we are interested only in CPs with successful updates from that user. Secondly, note that, in the evaluation of (37), we need to account for the statistical dependence between X and Y . In fact, the duration of the CP over which the last update was received does influence the number of users contending on the subsequent one, impacting both the probability for the user of interest to transmit and be decoded as well as the duration of the subsequent CPs.

It is therefore convenient to compute the statistical moments in (37) by conditioning on the system time. Let us start by considering the term $\mathbb{E}[XY]$, which we expand as

$$\mathbb{E}[XY] = \sum_{x=1}^{d_{\max}} x \cdot \mathbb{E}[Y | X = x] P_X(x). \quad (39)$$

Without loss of generality, let us denote by $\ell = 1$ the index of the first CP that contributed to the inter-update time being tracked. Accordingly, we reformulate the conditional expectation in (39) considering the value of $Z^{(1)}$ as

$$\mathbb{E}[Y | X = x] = \sum_z \mathbb{E}[Y | Z^{(1)} = z, X = x] \mathbb{P}\{Z^{(1)} = z | X = x\} \quad (40)$$

$$= \sum_z \mathbb{E}[Y | Z^{(1)} = z] \mathbb{P}\{Z^{(1)} = z | X = x\} \quad (41)$$

where the summation is taken over all the possible states $z = (d, s)$, $d \in \{1, \dots, d_{\max}\}$, $s \in \{0, 1\}$, and (41) follows from the Markov property of the involved processes. Note that the factors $\mathbb{P}\{Z^{(1)} = z | X = x\}$ on the right-hand side of (41) can be computed using (35) and (36).

The conditional expectation $\mathbb{E}[Y | Z^{(1)} = z]$ can be derived by resorting to a first step analysis [39]. To this aim, consider first the situation in which the packet from the user of interest is decoded already in the initial CP. In this case, Y coincides with the length of the initial CP:

$$\mathbb{E}[Y | Z^{(1)} = (d, 1)] = d. \quad (42)$$

When $Z^{(1)} = (d, 0)$ instead, the inter-update time can be computed as the sum of the durations of all CPs until the next update decoding. This can be conveniently computed by conditioning on the outcome of the first transition. Specifically,

$$\mathbb{E}[Y | Z^{(1)} = (d, 0)] = d + \sum_z \mathbb{E}[Y | Z^{(1)} = z] \cdot p_Z((d, 0), z) \quad (43)$$

where the Markov property ensures that the average duration, once the transition to state z has occurred, is equal to the one that we would have by starting from such state. Combining (42) and (43), we obtain a full-rank system of d_{\max} equations in the d_{\max} unknowns $\mathbb{E}[Y | Z^{(1)} = (d, 0)]$. Substituting the solutions of this system into (41), we obtain $\mathbb{E}[Y | X = x]$, which eventually allows us to compute $\mathbb{E}[XY]$ via (39). We also note that the availability of $\mathbb{E}[Y | X = x]$ allows us to evaluate the denominator of (37) via

$$\mathbb{E}[Y] = \sum_{x=1}^{d_{\max}} \mathbb{E}[Y | X = x] P_X(x). \quad (44)$$

The final term required to evaluate $\bar{\Delta}$ in (37) is $\mathbb{E}[Y^2]$. As before, we compute first the conditional expectation of Y^2 given $Z^{(1)}$ via a first-step analysis. This yields the following system of linear equations:

$$\mathbb{E}[Y^2 | Z^{(1)} = (d, 1)] = d^2 \quad (45)$$

and

$$\begin{aligned} \mathbb{E}[Y^2 | Z^{(1)} = (d, 0)] &= d^2 + 2d \sum_z \mathbb{E}[Y | Z^{(1)} = z] \cdot p_Z((d, 0), z) \\ &+ \sum_z \mathbb{E}[Y^2 | Z^{(1)} = z] \cdot p_Z((d, 0), z) \end{aligned} \quad (46)$$

where the terms $\mathbb{E}[Y | Z^{(1)} = z]$ were derived earlier. Solving this full-rank system of equation, we obtain the desired conditional second-order moments of Y , from which we compute $\mathbb{E}[Y^2]$ via

$$\mathbb{E}[Y^2] = \sum_{x=1}^{d_{\max}} \mathbb{E}[Y^2 | X = x] P_X(x). \quad (47)$$

The average AoI $\bar{\Delta}$ is then obtained by simply inserting (39), (44), and (47) into (37).

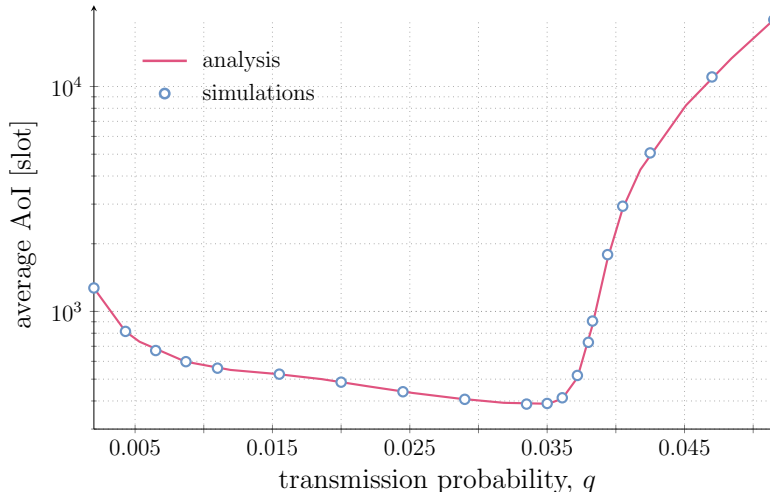


Fig. 6. Average node AoI $\bar{\Delta}$ vs transmission probability q . A population of $U = 200$ users and a maximum CP duration of $d_{\max} = 250$ slots are considered. The packet generation probability is set so that $\gamma U = 0.8$.

B. Numerical Results

1) *Throughput-AoI trade-off*: Leaning on the exact analysis presented so far, we illustrate the protocol behavior in terms of information freshness in Fig. 6, where we report the average AoI as a function of the channel access probability q . The same setting used for the throughput study of Fig. 3 is considered, i.e., $U = 200$ nodes, a maximum CP duration of $d_{\max} = 250$ slots, and an activation probability such that $\gamma U = 0.8$. In the plot, the solid lines denote analytical results, whereas markers denote the outcome of Monte Carlo simulations. We see from the figure that too low or too high values of q result in poor performance in terms of AoI. In the former case, an excessively conservative transmission behavior is likely to result in a user missing opportunities to deliver a status update: a user may end up not transmitting for the whole duration of a CP even when a packet is available. Conversely, when users become too aggressive, collisions dominate, hindering the capability of the receiver to decode transmitted updates prior to reaching the maximum contention duration.

By comparing Fig. 3 and Fig. 6, we see that the optimal operating points in terms of throughput and average AoI coincide. More generally, for a given traffic profile (U, γ) , and a given maximum CP duration, there exists a value q^* of the transmission probability that jointly maximizes S and minimizes $\bar{\Delta}$. This outcome is common to other random access solutions under symmetric traffic conditions, as epitomized by the inverse proportionality of AoI and throughput exhibited by

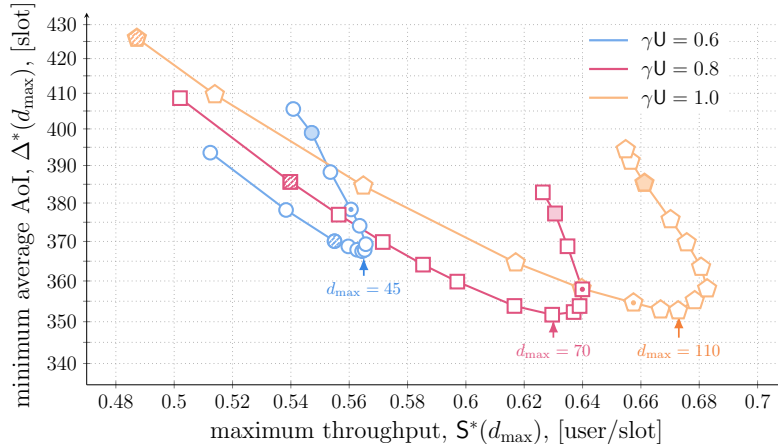


Fig. 7. Maximum throughput and minimum average AoI obtained when varying the maximum CP duration d_{\max} . Different lines correspond to results obtained for different values of γU ; in all cases $U = 200$. Each point is obtained considering a different value of d_{\max} , and corresponds to the maximum throughput and the minimum AoI in such conditions, i.e., $S^*(d_{\max})$ and $\Delta^*(d_{\max})$. For $\gamma U = 0.6$, the range $10 \leq d_{\max} \leq 220$ is shown; for $\gamma U = 0.8$, $20 \leq d_{\max} \leq 220$; and for $\gamma U = 1.0$, $40 \leq d_{\max} \leq 220$. The arrows point to the configuration that minimizes the AoI in each case. For reference, striped markers indicate performance for $d_{\max} = 30$, markers filled with a point the case $d_{\max} = 100$, and color-filled markers denote $d_{\max} = 180$.

slotted ALOHA [12], [28]. From this standpoint, any choice of $q \neq q^*$ reducing the probability to deliver a status update would also be harmful in terms of information freshness. In the remainder, we shall refer to these optimal results as $S^*(d_{\max}) = \max_q S(q, d_{\max})$ and $\Delta^*(d_{\max}) = \min_q \Delta(q, d_{\max})$, explicitly pointing out that the quantities are a function of the CP duration.

It is indeed interesting to observe that frameless ALOHA exhibits a more complex behavior when performance are analyzed versus d_{\max} . To explore this aspect, we report in Fig. 7 the throughput and average AoI pairs that can be achieved by tuning the maximum CP duration. Specifically, we consider different values of d_{\max} , pick, for each setting, the optimal access probability q^* , and plot $S^*(d_{\max})$ and $\Delta^*(d_{\max})$. The three different curves in the figure refer to three different packet generation probabilities $\gamma U \in \{0.6, 0.8, 1.0\}$, with $U = 200$. The lines illustrated our analytical results, whereas the markers correspond to simulation outcomes. The d_{\max} intervals studied for each case are available in the figure caption, whereas the results obtained for three reference values, $d_{\max} = 30$, $d_{\max} = 100$, $d_{\max} = 180$ are highlighted by special markers. Moreover, the maximum CP duration leading to the minimum possible AoI for each traffic generation level is explicitly reported in the plot for convenience.

Consider first the case $\gamma U = 0.8$, identified by the red curve (square markers) in Fig. 7, and

focus on throughput performance. For low values of d_{\max} , the system operates in the left region of the plot, providing low throughput. In this case, too short CPs hinder packet decoding, not allowing enough slots for SIC to be fully efficient. By increasing the maximum duration of the CP, we can improve the throughput and approach the elbow exhibited by the curve. After a certain point, though, a further increase of d_{\max} allows for the decoding of only a limited additional number of users, and such diminishing-return behavior leads to a decrease in throughput. Notably, while a similar trend emerges also for the average AoI, the impact of operating over excessively long CPs is far more pronounced. The rationale behind this lies in the dependency of $\bar{\Delta}$ on the inter-update time, i.e., the number of CPs between two updates as well as their duration in slots. From this standpoint, higher values of d_{\max} may reduce the former (increasing throughput), yet entail a larger average cost in terms of elapsed slots over a CP. While initially the first factor prevails, and $\bar{\Delta}$ improves together with S , the impact of longer CPs quickly turns out to be detrimental in terms of AoI.

The analysis reveals then a fundamental trade-off between information freshness and throughput, and implies that, for a given traffic generation rate, operating the system at maximum throughput entails a degradation of performance in terms of AoI. Such a behavior departs significantly from the one observed in plain ALOHA [12], and pinpoints a characteristic behavior of modern random access schemes employing SIC, first observed in [28] for irregular repetition slotted ALOHA.

Similar results can be observed for $\gamma U = 0.6$ and $\gamma U = 1.0$, with the discussed effect becoming more pronounced for higher traffic. Furthermore, longer CPs are needed to achieve better performance when γU increases, as the SIC process benefits from additional slots under harsher channel contention. Indeed, the maximum throughput is attained for $d_{\max} = 60$ slots when $\gamma U = 0.6$ but for $d_{\max} = 130$ slots when $\gamma U = 1.0$. A trade-off between $\bar{\Delta}$ and S emerges also when one looks at the nodes activation probability. Indeed, while the highest throughput among the considered setups is attained for $\gamma U = 1.0$, the best results in terms of information freshness is achieved for the lower level of contention $\gamma U = 0.8$.

To conclude our discussion, we present a performance comparison among frameless ALOHA and two benchmarks: a baseline slotted ALOHA scheme, and irregular repetition slotted ALOHA (IRSA) [17]. For slotted ALOHA, we assume that a node immediately sends a newly generated update, without retransmissions, resulting in a probability of accessing the channel at each slot of γ . For the collision channel model under study, this leads to the classical throughput

expression [40]

$$S_{sa} = \gamma U (1 - \gamma)^{U-1}. \quad (48)$$

Similarly, the average AoI can be expressed in closed form as [12], [28]

$$\bar{\Delta}_{sa} = \frac{1}{2} + \frac{U}{S_{sa}}. \quad (49)$$

Note that both metrics are optimized, i.e., maximum throughput, minimum AoI, when the system operates at a channel load of 1 packet per slot, i.e., corresponding to $\gamma U = 1$.

On the other hand, IRSA is a well-known benchmark for modern random access schemes [41], and operates similar to frameless ALOHA. Indeed, both protocols rely on having users transmit multiple copies of a packet and on the use of SIC to resolve collisions. The main difference lies in the fact that a contention period in frameless ALOHA can be terminated by the receiver as soon as all users are decoded, whereas with IRSA the predefined end of the frame will always be reached. We refer the interested reader to [17] for a detailed description of the operation procedures. Thanks to its ability to adaptively terminate the contention, frameless ALOHA is capable to improve throughput performance over IRSA [24].⁷ In turn, this feature can intuitively be beneficial also in terms of age of information, reducing the time between successive updates that a node can perform. To explore this aspect, we lean on the average IRSA AoI derivation in [28]. To grant a fair comparison with the setup under study, we assume that a transmitted packet has time stamp set to the start instant of the frame, and obtain

$$\bar{\Delta}_{irsa} = \frac{d}{2} + \frac{U}{S} \quad (50)$$

where d is the number of slots composing a frame and S_{irsa} is the protocol throughput. The result in (50) highlights the important role played by the frame duration in IRSA. On the one hand, operating the protocol with longer frames can lead to better throughput performance [17], [28], lowering the second component of $\bar{\Delta}_{irsa}$ in (50). On the other hand, larger values of d contribute linearly to the growth of the first addend.

The performance of the three schemes is compared in Fig. 8, which reports the average AoI against the throughput for two different values of γ , i.e. $\gamma U = 0.6$ and $\gamma U = 1.0$. For frameless

⁷We note that these benefits come at the cost of a more frequent feedback, distributed by the receiver after each contention period. In this respect, IRSA can be less demanding, as sporadic beacons sent to the users can be sufficient to maintain frame alignment over time.

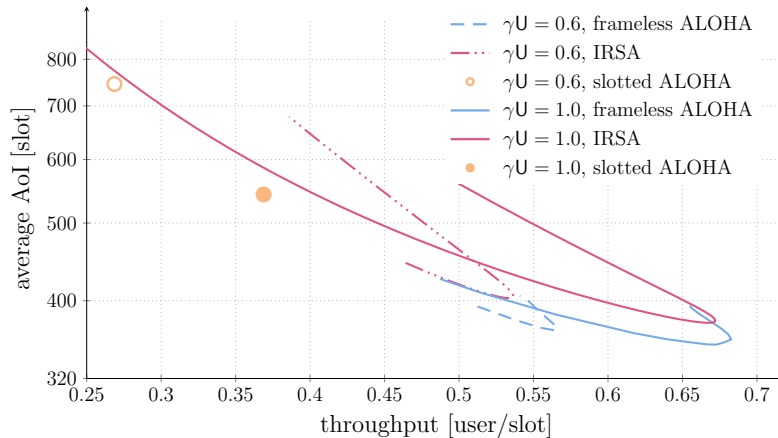


Fig. 8. Average AoI vs aggregate throughput for IRSA (magenta lines), frameless ALOHA (blue lines) and slotted ALOHA (circle markers) for two traffic generation intensities ($\gamma U = 0.6$ and $\gamma U = 1.0$). In all cases, $U = 200$ users were considered. For IRSA, a replica distribution $\Lambda(x) = 0.86x^3 + 0.14x^8$ [42] was used, and each point in the curves denotes performance attained for a different frame duration, ranging between 30 and 350 slots. For frameless ALOHA, $S^*(d_{\max})$ and $\Delta^*(d_{\max})$ are shown, varying the maximum frame duration d_{\max} .

ALOHA, results were obtained by varying the maximum contention period duration d_{\max} , and the points report $\Delta^*(d_{\max})$ and $S^*(d_{\max})$, akin to what done in Fig. 7. As to IRSA, the protocol was operated using a replica distribution $\Lambda(x) = 0.86x^3 + 0.14x^8$ [42], i.e., each node attempting transmission over a frame sends 3 copies of its packet over the d slots with probability 0.86, whereas 8 copies are sent with probability 0.14. The curves show the performance for values of d ranging from 30 to 350 slots. Finally, the performance of slotted ALOHA is denoted by an empty ($\gamma U = 0.6$) or filled ($\gamma U = 1.0$) marker, whose coordinates are computed via (48) and (49).

As expected, Fig. 8 highlights that both advanced schemes clearly outperform the basic random access solution. More interestingly, frameless ALOHA improves over IRSA in both traffic configurations. Specifically, let us consider the minimum average AoI that the schemes can obtain when varying the contention duration. The plot shows that a metric reduction of $\sim 10\%$ and $\sim 7\%$ is achieved for $\gamma U = 0.6$ and $\gamma U = 1.0$, respectively. Notably, when the protocols are operated in these configurations, they offer very similar throughput. In other words, frameless ALOHA is capable of improving AoI without undergoing a penalty in terms of throughput when compared to IRSA. Along a similar line, one may want to operate the schemes so that throughput is maximized. In this situation, frameless ALOHA offers a minor throughput improvement of $\sim 5\%$ and $\sim 2\%$ for $\gamma U = 0.6$ and $\gamma U = 1.0$, respectively. However, the average AoI in these

TABLE I

PERFORMANCE COMPARISON OF SLOTTED ALOHA, IRREGULAR REPETITION SLOTTED ALOHA (IRSA) [17] AND FRAMELESS ALOHA, IN TERMS OF THE MAXIMUM ACHIEVABLE THROUGHPUT \hat{S} AND THE MINIMUM ACHIEVABLE AVERAGE AOI $\hat{\Delta}$ FOR DIFFERENT VALUES OF γU . FOR FRAMELESS ALOHA (IRSA), THE MAXIMUM CP DURATION (FRAME DURATION) ATTAINING THE REPORTED RESULTS IS ALSO GIVEN IN PARENTHESES. IN ALL CASES, $U = 200$.

	$\gamma U = 0.4$		$\gamma U = 0.6$		$\gamma U = 0.8$		$\gamma U = 1.0$	
	\hat{S} [pkt/slot]	$\hat{\Delta}$ [slot]	\hat{S} [pkt/slot]	$\hat{\Delta}$ [slot]	\hat{S} [pkt/slot]	$\hat{\Delta}$ [slot]	\hat{S} [pkt/slot]	$\hat{\Delta}$ [slot]
slotted ALOHA	0.2686	745.22	0.3300	606.59	0.3603	555.55	0.3688	542.79
IRSA (d)	0.3838 (35)	537.65 (31)	0.5364 (65)	403.0279 (56)	0.6278 (113)	372.3377 (103)	0.6721 (160)	375.4708 (151)
frameless ALOHA (d_{\max})	0.3987 (30)	503.54 (30)	0.5657 (60)	367.46 (45)	0.6399 (100)	351.67 (70)	0.6827 (130)	352.67 (110)

settings is reduced by $\sim 9\%$ and $\sim 5\%$. Also in such operating conditions, therefore, resorting to frameless ALOHA can be beneficial.

The outcomes of Fig. 8 are complemented by Table I, pinpointing the optimal results that can be obtained by the three considered protocols for four different values of γU . The values reported for frameless ALOHA correspond to the maximum attainable throughput \hat{S} and minimum attainable average AoI $\hat{\Delta}$ that can be achieved by tuning d_{\max} . Specifically, the results were obtained by optimizing over both the maximum CP duration and the transmission probability q , leading to $\hat{S} = \max_{d_{\max}} S^*(d_{\max})$ and $\hat{\Delta} = \min_{d_{\max}} \Delta^*(d_{\max})$. The value of d_{\max} under which the shown performances are achieved (in general different for throughput and AoI) is also noted for completeness. Similarly, for IRSA, we report the optimal values for AoI and throughput obtained among all the considered frame durations. The improvements triggered by frameless ALOHA are apparent from the table, with an average AoI almost halved ($\sim 60\%$) compared to that of slotted ALOHA, and throughput gains up to 90%. We remark that such results are obtained simply by optimizing over the pair (d_{\max}, q) . From this standpoint, the frameless approach offers additional room for improvements, which may pave the road for further gains. As an example, we provide next some initial considerations on how a dynamic adaptation of the maximum CP duration may be leveraged to improve both AoI and throughput.

C. Performance Improvements via Early Termination of Contention Period

It was shown in [29] that terminating the CP after having decoded only a fraction of the contending users can be beneficial, at least in terms of throughput. The purpose of this section is to investigate whether introducing such a termination criterion is also beneficial in terms of average AoI. In particular, in this section we compare two different contention termination strategies. The first one (baseline) is the one we considered so far, i.e., the CP is terminated after all users are decoded or after d_{\max} slots have elapsed since the beginning of the CP. The second strategy, inspired by [29], entails terminating the CP whenever the fraction of decoded users reaches 0.85 or after a total of d_{\max} slots have elapsed. We refer to this strategy as *early termination*. Note that this strategy requires the receiver to know the number of contending users. As argued in [38], the number of contending users can be estimated from the number of idle, singleton, and collided slots.

In Fig. 9, we show the maximum throughput $S^*(d_{\max})$ and minimum average AoI $\Delta^*(d_{\max})$ for a setup with $U = 200$ users and $\gamma U = 0.8$ for the two CP termination strategies, and for values of d_{\max} between 20 and 220 slots. Note that, for small values of d_{\max} (upper left region of the plot), terminating the CP before decoding all users is detrimental both in terms of throughput and average AoI. On the contrary, for larger values of d_{\max} , this strategy is beneficial for both performance metrics. The intuition behind these results is the following. Consider a contention period in which a fraction f of the contending users is still unresolved. Let us consider two different groups of users: the first group contains the unresolved contending users, whereas the second group contains the pending users, i.e., the users who have an update to send in the next contention period. In terms of AoI, for the first group (unresolved users) it is beneficial to continue the contention so that these users have a chance of delivering a successful update. In contrast, for the second group (pending users) it is beneficial in terms of AoI to terminate the current contention so that they can immediately start contending to deliver their update. For small contention periods, it is better not to apply early termination, since the benefit of giving unresolved users the chance of successfully delivering an update outweighs the penalty incurred by having the pending users wait. In contrast, for large values of d_{\max} , once a substantial fraction of the users is resolved (e.g., 0.85), it is better to terminate early the contention, so that pending users can immediately start contending to send their updates (although we condemn unresolved users to wait until their next update to reset their age).

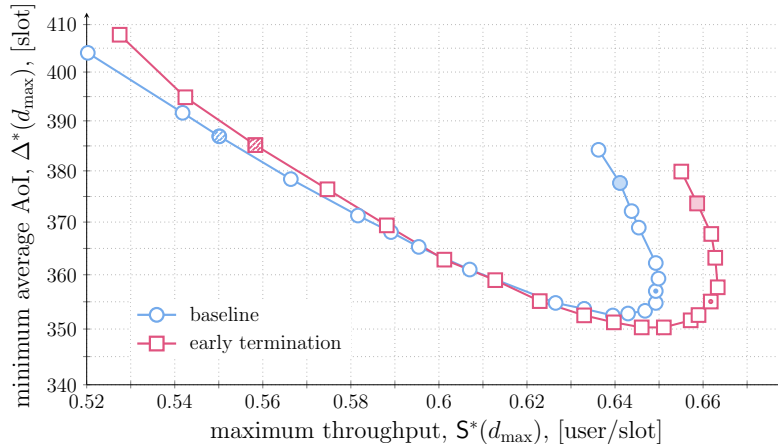


Fig. 9. Maximum throughput and minimum average AoI obtained when varying the maximum CP duration d_{\max} , for $\gamma U = 0.8$ and $U = 200$. Circle markers denote the baseline strategy where the contention is terminated after all contending users are decoded or after the maximum contention duration d_{\max} is reached. In turn, the square markers represent an early-termination strategy inspired by [29], in which the CP is terminated after at least 85% of the contending users are decoded or after d_{\max} slots have elapsed. For reference, striped markers indicate performance for $d_{\max} = 30$, markers filled with a point the case $d_{\max} = 100$, and color-filled markers denote $d_{\max} = 180$.

VI. CONCLUSIONS

We studied the dynamic behavior of frameless ALOHA, focusing on the throughput and the age of information (AoI) performance. The analysis is based on a finite-length analysis of the successive interference cancellation process of frameless ALOHA, and on a Markovian analysis of the system state evolution. We characterized the stability of the protocol via a drift analysis, which allowed us to determine the presence of stable and unstable equilibrium points. Finally, we provided an exact characterization of the AoI performance, based on which we unveiled the impact of some key protocol parameters such as the maximum length of the contention period, on the average AoI. Our results indicate that configurations of parameters that maximize the throughput may result in a degradation of the AoI performance.

REFERENCES

- [1] A. Munari, F. Lázaro, G. Durisi, and G. Liva, “An age of information characterization of frameless ALOHA,” in *Proc. Asilomar Conference on Signals, Systems and Computers*, Nov. 2021.
- [2] R. D. Yates, Y. Sun, D. R. Brown, S. K. Kaul, E. Modiano, and S. Ulukus, “Age of information: An introduction and survey,” *IEEE J. Sel. Areas Commun.*, vol. 39, no. 5, pp. 1183–1210, May 2021.

- [3] E. Uysal, O. Kaya, A. Ephremides, J. Gross, M. Codreanu, P. Popovski, M. Assaad, G. Liva, A. Munari, B. Soret, T. Soleymani, and K. H. Johansson, “Semantic communications in networked systems: A data significance perspective,” *IEEE Network*, vol. 36, no. 4, pp. 233–240, Oct. 2022.
- [4] S. Kaul, M. Gruteser, V. Rai, and J. Kenney, “Minizing age of information in vehicular networks,” in *Proc. IEEE SECON*, June 2011.
- [5] S. Kaul, R. Yates, and M. Gruteser, “Real-time status: How often should one update?” in *Proc. IEEE INFOCOM*, Mar. 2012.
- [6] O. Ayan, M. Vilgelm, M. Klügel, S. Hirche, and W. Kellerer, “Age-of-information vs. value-of-information scheduling for cellular networked control systems,” in *Proc. ACM/IEEE ICCPS*, Apr. 2019.
- [7] Y. Sun, Y. Polyanskiy, and E. Uysal, “Sampling of the Wiener process for remote estimation over a channel with random delay,” *IEEE Trans. Inf. Theory*, vol. 66, no. 2, pp. 1118–1135, Feb. 2020.
- [8] N. Abramson, “The ALOHA System - Another alternative for computer communications,” in *Proc. 1970 Fall Joint Computer Conference*. AFIPS Press, Nov. 1970.
- [9] L. G. Roberts, “ALOHA packet systems with and without slots and capture,” *ARPANET System Note 8 (NIC11290)*, Jun 1972.
- [10] LoRa Alliance, “The LoRa Alliance wide area networks for Internet of things,” www.lora-alliance.org.
- [11] Sigfox, “SIGFOX: The global communications service provider for the Internet of things,” www.sigfox.com.
- [12] R. Yates and S. Kaul, “Status updates over unreliable multiaccess channels,” in *Proc. IEEE Int. Symp. Inf. Theory*, Jul. 2017.
- [13] —, “Age of information in uncoordinated unslotted updating,” in *Proc. IEEE Int. Symp. Inf. Theory*, Jun. 2020.
- [14] O. Yavascan and E. Uysal, “Analysis of slotted ALOHA with an age threshold,” *IEEE J. Sel. Areas Commun.*, vol. 39, no. 5, pp. 1456–1470, May 2021.
- [15] X. Chen, K. Gatsis, H. Hassani, and S. Bidokhti, “Age of information in random access channels,” *IEEE Trans. Inf. Theory*, vol. 68, no. 10, pp. 6548–6568, 2022.
- [16] E. Casini, R. De Gaudenzi, and O. del Rio Herrero, “Contention resolution diversity slotted ALOHA (CRDSA): An enhanced random access scheme for satellite access packet networks,” *IEEE Trans. Wireless Commun.*, vol. 6, no. 4, pp. 1408–1419, Apr. 2007.
- [17] G. Liva, “Graph-based analysis and optimization of contention resolution diversity slotted ALOHA,” *IEEE Trans. Commun.*, vol. 59, no. 2, pp. 477–487, Feb. 2011.
- [18] Y. Polyanskiy, “A perspective on massive random-access,” in *Proc. IEEE Int. Symp. Inf. Theory*, Jul. 2017.
- [19] S. S. Kowshik, K. Andreev, A. Frolov, and Y. Polyanskiy, “Energy efficient coded random access for the wireless uplink,” *IEEE Trans. Commun.*, vol. 68, no. 8, pp. 4694–4708, Aug. 2020.
- [20] V. K. Amalladinne, J.-F. Chamberland, and K. R. Narayanan, “A coded compressed sensing scheme for unsourced multiple access,” *IEEE Trans. Inf. Theory*, vol. 66, no. 10, pp. 6509–6533, Oct. 2020.
- [21] A. Decurninge, I. Land, and M. Guillaud, “Tensor-based modulation for unsourced massive random access,” *IEEE Wireless Commun. Lett.*, vol. 10, no. 3, pp. 552–556, Mar. 2021.
- [22] A. Fengler, P. Jung, and G. Caire, “SPARCs for unsourced random access,” *IEEE Trans. Inf. Theory*, vol. 67, no. 10, pp. 6894–6915, Oct. 2021.
- [23] K. R. Narayanan and H. D. Pfister, “Iterative collision resolution for slotted ALOHA: An optimal uncoordinated transmission policy,” in *Proc. Int. Symp. Turbo Codes and Iterative Inf. Process.*, Aug. 2012.
- [24] C. Stefanović, P. Popovski, and D. Vukobratovic, “Frameless ALOHA protocol for wireless networks,” *IEEE Commun. Lett.*, vol. 16, no. 12, pp. 2087–2090, Dec. 2012.

- [25] E. Paolini, G. Liva, and M. Chiani, "Coded slotted ALOHA: A graph-based method for uncoordinated multiple access," *IEEE Trans. Inf. Theory*, vol. 61, no. 12, pp. 6815–6832, Dec. 2015.
- [26] E. Sandgren, A. Graell i Amat, and F. Brännström, "On frame asynchronous coded slotted ALOHA: Asymptotic, finite length, and delay analysis," *IEEE Trans. Commun.*, vol. 65, no. 2, pp. 691–703, Feb. 2017.
- [27] F. Clazzer, C. Kissling, and M. Marchese, "Enhancing contention resolution ALOHA using combining techniques," *IEEE Trans. Commun.*, vol. 66, no. 6, pp. 2576–2587, 2018.
- [28] A. Munari, "Modern random access: an age of information perspective on irregular repetition slotted ALOHA," *IEEE Trans. Commun.*, vol. 69, no. 6, pp. 3572–3585, Jun. 2021.
- [29] C. Stefanović and P. Popovski, "ALOHA random access that operates as a rateless code," *IEEE Trans. Commun.*, vol. 61, no. 11, pp. 4653–4662, Nov. 2013.
- [30] R. Gallager, "Low-density parity-check codes," Ph.D. dissertation, Massachusetts Institute of Technology, Cambridge, MA, USA, 1963.
- [31] M. Luby, "LT codes," in *Proc. IEEE Symp. Found. Comp. Sci.*, Vancouver, Canada, Nov. 2002, pp. 271–282.
- [32] F. Lázaro, C. Stefanović, and P. Popovski, "Reliability-latency performance of frameless ALOHA with and without feedback," *IEEE Trans. Commun.*, vol. 68, no. 10, pp. 6302–6316, Oct. 2020.
- [33] R. Karp, M. Luby, and A. Shokrollahi, "Finite length analysis of LT codes," in *Proc. IEEE Int. Symp. Inf. Theory*, Jun. 2004.
- [34] L. Kleinrock and S. Lam, "Packet switching in a multiaccess broadcast channel: Performance evaluation," *IEEE Trans. Commun.*, vol. 23, no. 4, pp. 410–423, Apr. 1975.
- [35] S. Lam and L. Kleinrock, "Packet switching in a multiaccess broadcast channel: Dynamic control procedures," *IEEE Trans. Commun.*, vol. 23, no. 9, pp. 891–904, Sep. 1975.
- [36] R. D. Yates and S. K. Kaul, "The age of information: Real-time status updating by multiple sources," *IEEE Trans. Inf. Theory*, vol. 65, no. 3, pp. 1807–1827, March 2019.
- [37] D. Bertsekas and R. G. Gallager, *Data networks*. Upper Saddle River, NJ, USA: Prentice-Hall, Inc., 1987.
- [38] C. Stefanović, K. F. Trilingsgaard, N. K. Pratas, and P. Popovski, "Joint estimation and contention-resolution protocol for wireless random access," in *Proc. IEEE Int. Conf. Commun.*, Jun. 2013.
- [39] H. Taylor and S. Karlin, *An introduction to stochastic modeling*, 3rd ed. London: Academic Press, 1998.
- [40] N. Abramson, "The throughput of packet broadcasting channels," *IEEE Trans. Commun.*, vol. COM-25, no. 1, pp. 117–128, 1977.
- [41] M. Berioli, G. Cocco, G. Liva, and A. Munari, "Modern random access protocols," *Foundations and Trends® in Networking*, vol. 10, no. 4, pp. 317–446, 2016.
- [42] A. Graell i Amat and G. Liva, "Finite-length analysis of irregular repetition slotted ALOHA in the waterfall region," *IEEE Commun. Letters*, vol. 22, no. 5, pp. 886–889, 2018.